Available online at www.sciencedirect.com
ScienceDirect
Trans. Nonferrous Met. Soc. China 33(2023) 1258−1270
Transactions of Nonferrous Metals Society of China
www.tnmsc.cn

Effect of injection of different gases on removal of arsenic in form of dust from molten copper smelting slag prior to recovery process

Hong-yang WANG[1,2], Rong ZHU[1,2], Kai DONG[1,2], Si-qi ZHANG[3], Yun WANG[4], Xin-yi LAN[5]

1. School of Metallurgical and Ecological Engineering,
University of Science and Technology Beijing, Beijing100083, China;
2. Beijing Key Laboratory for Special Melting and Preparation of High-end Metal Materials,
University of Science and Technology Beijing, Beijing100083, China;
3. School of Civil and Resources Engineering, University of Science and Technology Beijing, Beijing100083, China;
4. The China ENFI Engineering Co., Ltd., Beijing100038, China;
5. School of Automation and Electrical Engineering,
University of Science and Technology Beijing, Beijing100083, China

Received 1 December 2021; accepted 8 July 2022

Abstract: In order to reduce the environmental risks caused by arsenic in copper smelting slag, a method of dearsenisation from molten slag based on gas injection was proposed. It was expected to enrich arsenic in the form of dust prior to copper recovery process. The effects of inert, oxidising, and reducing gas on the removal of arsenic from molten slag were compared. When CO_2 was injected, the removal of arsenic was mainly attributed to the oxidation of Cu–As inclusions and arsenic sulphide in the slag. Based on the injection of CO, the removal rate of arsenic reached more than 60%. Based on the injection of reducing gas, arsenic oxide in the FeO_x−SiO_2 slag was reduced and volatilised into the gas phase, resulting in the removal of arsenic. This study provides a reference with respect to the establishment of strategies for the mitigation of arsenic pollution caused by smelting slag.

Key words: copper smelting slag; dearsenisation; gas injection; pollutant control

1 Introduction

Copper smelting slag (smelting slag) is a solid waste produced during copper smelting. It contains a large number of metals and thus has a high recycling value [1,2]. Based on the widespread use of copper concentrates, a large number of arsenic-containing pollutants and by-products are produced [3−7]. During copper smelting, a large amount of arsenic is enriched in the slag. Because of the different compositions of copper concentrates, the arsenic concentration in smelting slag generally ranges from 0.1% to 1% [8,9].

After flotation, the copper content can be reduced to less than 0.35%. However, it is difficult to simultaneously separate copper and arsenic in the flotation process. When copper is recovered, a large amount of arsenic is concentrated in the slag, which cannot be effectively separated [10−12]. The trace element arsenic is dissolved in multiple phases of the copper slag; therefore, the affinity of different arsenic compounds to solvents makes it difficult to reduce its content to a very low value [13,14]. The environmental risk of arsenic in tailings cannot be ignored.

The pyrometallurgical reduction smelting is another effective method to treat copper slag. Based

Corresponding author: Kai DONG, Tel: +86-17710349134, E-mail: dongkai0015@163.com
DOI: 10.1016/S1003-6326(23)66180-1

on this method, the copper content in the slag can be reduced to 0.5%. Although the copper recovery efficiency in pyrometallurgical reduction is lower than that of the flotation process, it can be used to directly treat molten copper slag with greater raw material adaptability [15−17]. During the pyrometallurgical reduction, arsenic in the slag is enriched in reduction products or volatilised in the form of dust and stripped from the slag [18]. However, many problems can occur during the reduction. Most of the arsenic is recycled based on the reuse of products (matte, metal) [14], which leads to the accumulation in the process.

For arsenic in dust, both roasting and hydro-extraction are cost-effective and have a high separation ability [19−25]. If arsenic in the copper slag is enriched in dust, arsenic can be separated from the slag, the arsenic recovery can be improved, and the arsenic content in tailings and environmental risk can be reduced. The volatilisation and enrichment of elements in molten copper slag are generally studied together with the pyrometallurgical smelting reduction process.

A pretreatment method can be proposed to remove arsenic from the molten slag in the form of dust prior to flotation or smelting reduction in the recovery process. The pretreatment can be connected with the slag discharge process of the smelting furnace and carried out in an electric furnace [2], but it must be separated from the pyrometallurgical process (reduction and melting separation). This assumption is illustrated in Fig. 1. Combined with the above-mentioned analysis, the use of gas injection should be considered to enrich arsenic from molten copper slag as dust via pretreatment. Inert, oxidising, and reducing gas can be used for the predearsenisation process.

At present, the selection of gas and the effect of various gases on the arsenic removal have not been analysed in detail. Inert gas, oxidizing gas, and reducing gas can be considered as arsenic removal media. However, the oxidation of air is strong, and a large amount of magnetite precipitation, which affects the fluidity of molten pool, may have an adverse impact on the removal of arsenic. In this study, in order to avoid metal formation as much as possible and maintain good fluidity of slag during injection, CO_2 and CO were selected as oxidizing gas and reducing gas, respectively. The effects of different gases on the arsenic removal are discussed. The XRD, EPMA, and XPS were used to analyse the distribution and morphology of arsenic in silicate, matte, and dust. The removal mechanism, arsenic volatilisation, is discussed. Based on our findings, we proposed the subsequent methods for utilisation of molten copper slag.

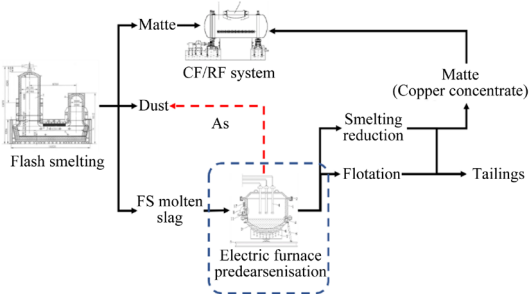

Fig. 1 Process overview of predearsenisation

2 Experimental

2.1 Raw material

Copper slag from flash smelting was selected for the experiment. Its chemical composition is listed in Table 1. The Fe/SiO_2 ratio of the slag is 1.86 and the copper content is high. The composition is complex, and the slag contains many impurities. Therefore, it can be used as a typical sample for experimental studies. Because the composition of industrial slag varies, the test copper slag was crushed in advance and fully mixed and the average value of three measurements was used.

Table 1 Chemical composition of copper slag (wt.%)

Cu	Fe	As	S	CaO	MgO
4.83	42.16	0.69	2.38	1.96	2.09
SiO_2	Al_2O_3	Pb	Zn	Sb	
22.66	3.93	0.91	3.56	1.05	

The microstructure of the copper slag was analysed using SEM−EDS. Figure 2 shows that there is a small amount of matte in the copper slag, which is the main form of copper. The Fe_3O_4 precipitation is evenly distributed in the copper slag because the reaction of industrial copper slag is incomplete and in a non-equilibrium state. Figure 2 shows that the copper slag mainly includes an iron-rich phase and a small amount of a copper-rich phase. Large iron-rich phases are mainly composed of magnetite [26] with diameters ranging from 10 to

30 μm. The excellent fluidity of molten pool is expected in the process of arsenic removal. A large amount of magnetite in the copper slag leads to an increase in the melting point (This refers specifically to the melting point of the complete liquid phase). Referring to our previous research, 1400 °C was selected as the experimental temperature [27]. In addition, the slag has a better fluidity at this temperature, ensuring the efficient removal of arsenic.

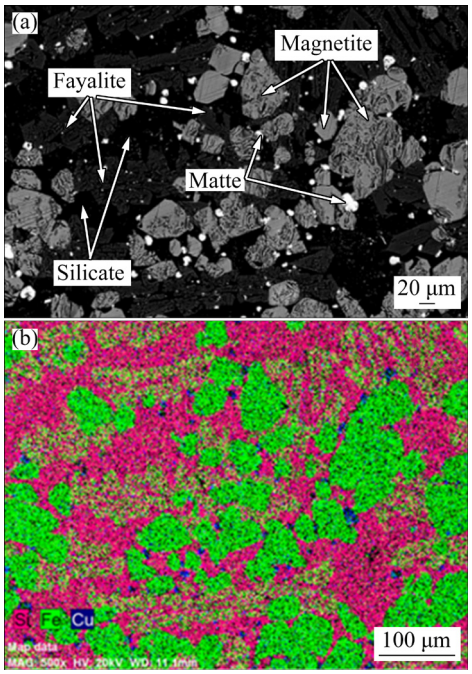

Fig. 2 BSD image (a) and EDS mapping (b) of copper slag

2.2 Experimental procedure

The main experiment equipment was a high-temperature tube furnace with a controlled atmosphere and temperature control accuracy of ±1 °C (Fig. 3). When the temperature reached the target temperature of 1400 °C, the gas injection was initiated after holding for 30 min. This time was regarded as the zero point of the injection. After the injection, the crucible was removed for water cooling (the molten sample has not been quenched with water, and phase precipitation still occurred during the cooling process). After the crucible was broken into large pieces, the matte at the bottom of the crucible was separated from the slag [27]. Following the physical separation, the matte and slag were tested. As the slag surface of the upper part of the crucible might be oxidised in a small amount during cooling, the slag in the middle of the crucible was selected for subsequent analysis and characterization. During the experiment, the method of quench filter screen filtration was used to collect dust, and the collected dust was directly used for the subsequent characterization and analysis.

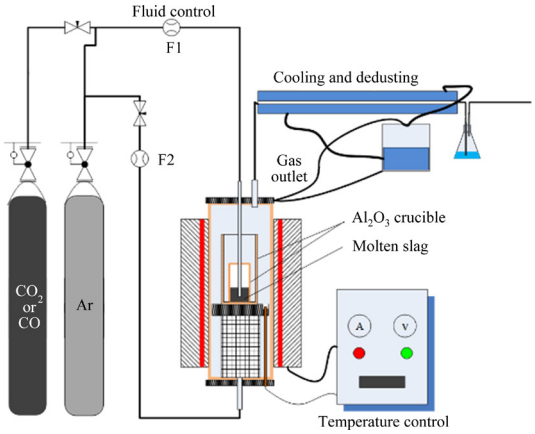

Fig. 3 Schematic diagram of experimental equipment

Arsenic volatilization is inevitable in the process of temperature rise, gas injection, and heat preservation [28]. To control the injection time of CO_2 and CO as unique variables, it is necessary to maintain a fixed heating rate and protective gas flow during the heating process. To distinguish the effects of different gases on the arsenic removal and eliminate uncertainty due to the injection time, it is necessary to ensure a fixed injection time after insulation. To ensure a total injection time of 40 min, after the injection of different oxidising and reducing gases, argon was injected to retain the total injection time unchanged. This experimental method is different from the previous experimental method used by the scholars to discuss the kinetic mechanism of a single species of gas [29]. The relationship of the temperature increase to the injection time is illustrated in Fig. 4. The injection time of CO_2 (CO) varied from 0 to 40 min. At the end of the gas injection period, argon was introduced to maintain the total injection time at 40 min. This injection experiment was carried out three times and the average value was used for the data analysis. It should be noted that the initial experimental results were the results from the argon injection for 40 min. Hereinafter, injection time refers to the actual injection time of CO_2 or CO.

The methods of analysis and characterization are provided in detail in the supplementary materials.

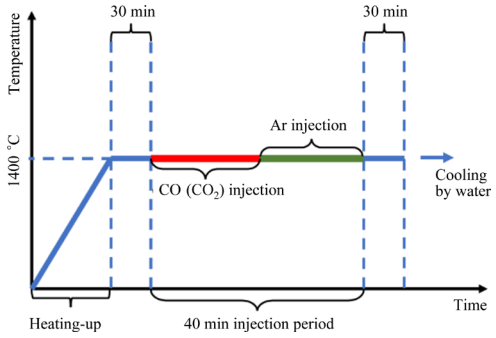

Fig. 4 Experimental operation

3 Results and analysis

3.1 Arsenic distribution and removal rate

The arsenic content of the slag changes depending on the injection of different gases, as shown in Fig. 5(a). During CO_2 injection, the arsenic content of the slag slowly and linearly decreases. In contrast, the arsenic content of the slag rapidly decreases during CO injection. When the arsenic content reaches ~0.13%, it remains unchanged. At this time, As_2O_3 reaches the removal limit and it is difficult to remove arsenic from the slag. Figure 5(b) shows that the arsenic content in the matte gradually decreases with increasing amount of injected CO_2, presenting a linear trend. The linear decrease of arsenic in the matte indicates that arsenic can be removed by the injection of CO_2. In contrast, with the increase in the amount of injected CO, the arsenic content of the matte increases and remains almost unchanged under excessive injection conditions.

The distributed mass of arsenic in each phase can be predicted by conversion, as shown in Fig. 6. With the increase in the CO_2 injection, the mass of arsenic in the slag and matte continuously decreases and shows a linear trend. The CO_2 injection promotes the removal of arsenic from the slag and matte. During CO injection, the proportion of arsenic entering the matte phase linearly increases, whereas the mass of arsenic removed by gasification slowly changes with the injection time and hardly enters the gas phase in the later stage. It can be concluded that a large amount of reduced arsenic in the slag is removed by the gas phase in the early stage of CO injection and a small amount of reduced arsenic is dissolved in the matte phase. However, as the reaction proceeds, As hardly enters the gas phase system by reducing after 24 min. The

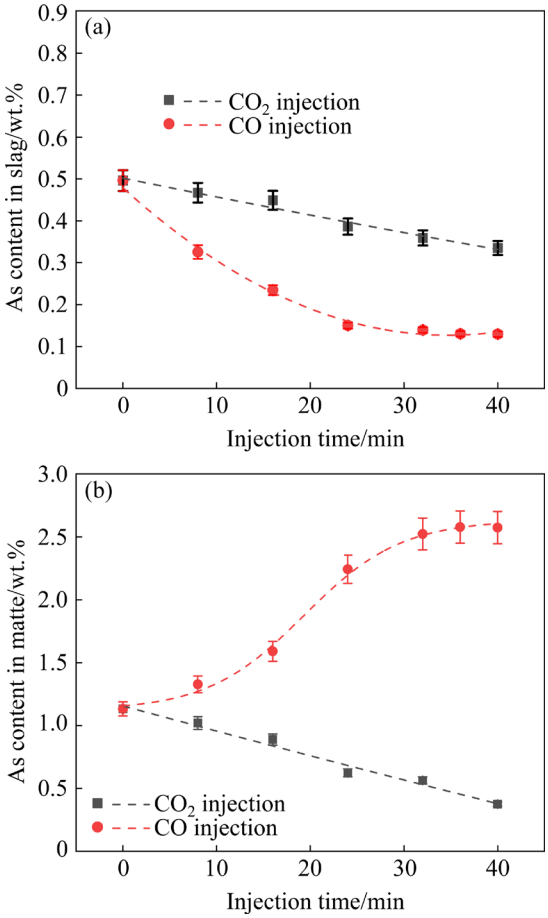

Fig. 5 Correlation between arsenic content of slag and injection time (a) and correlation between arsenic content of matte and injection time (b)

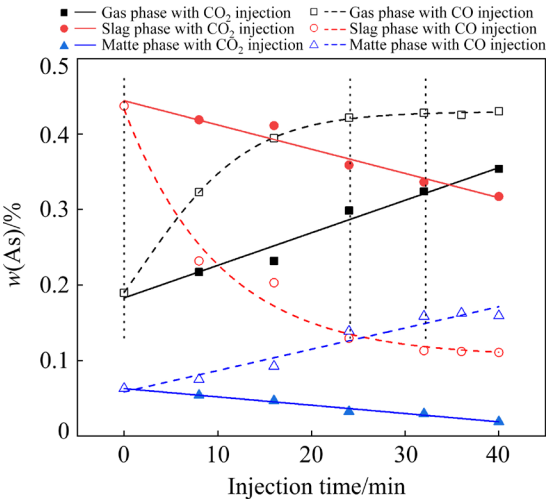

Fig. 6 Mass distribution of arsenic in various phases

As in the slag is reduced and dissolves in the matte phase in 24−32 min. When the injection time exceeds 32 min, CO cannot react with arsenic oxide in the copper slag continuously, and arsenic neither transfers to the gas phase nor dissolves in the matte phase.

As shown in Fig. 7, the removal rate of arsenic from the copper slag was calculated as a function of the gas injection time. Compared with pure argon injection, the removal rate of arsenic linearly increases with the CO_2 injection time and 51% of arsenic can be effectively removed. In contrast, under the action of CO, the removal rate of arsenic is significantly higher than that based on CO_2 injection and up to 62% of As is removed. In contrast to the linear growth of CO_2, the increase in the arsenic removal rate is notably slower after a CO injection time of 16 min. After 32 min, it is difficult to continue arsenic removal.

The arsenic distribution between the matte and slag varies depending on the injection time, as shown in Fig. 8. Based on the distribution ratio of arsenic, the removal efficiency decreases during CO injection, but the dissolution of arsenic in the matte phase is not inhibited. The distribution ratio of As (L_{As}) decreases during CO_2 injection, which indicates that residual arsenic accumulates in the FeO_x−SiO_2 slag.

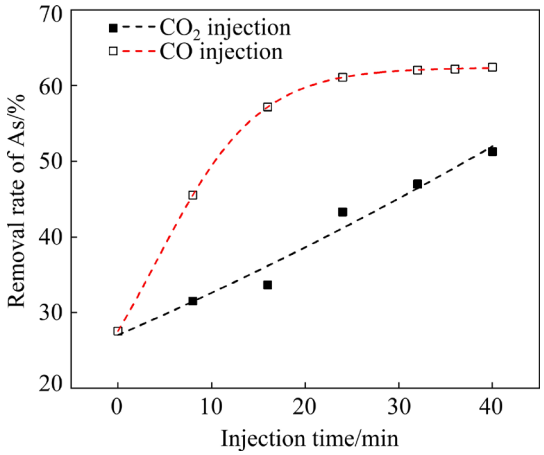

Fig. 7 Correlation between arsenic removal rate and injection time

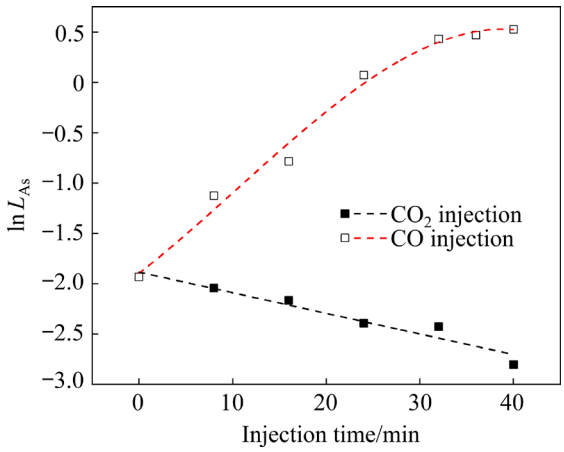

Fig. 8 Correlation between arsenic distribution ratio (L_{As}) and injection time

During CO injection, the transfer of arsenic to the matte is coupled with Cu, Fe, S, and other elements. The solubility of As and correlations between arsenic and other elements must be discussed. Based on the analysis of Cu, Fe, and S, the basic correlation between the slag and matte can be obtained under different gas injection conditions. Figure 9 shows that the Cu and S contents of the slag decrease with the increase in the gas injection time during CO_2 and CO injection, but the reaction mechanisms of these two processes completely differ. During CO_2 injection, the decrease in the Cu content is mainly caused by the following reaction:

$$Cu_2S+O_2=2Cu+SO_2 \quad (1)$$

The decrease in the Cu content during CO injection is caused by

$$Cu_2O+CO=2Cu+CO_2 \quad (2)$$

In the process of CO_2 injection, the reduction of S is mainly due to the oxidation of sulphur, whereas S is transferred from the slag to the matte during CO injection.

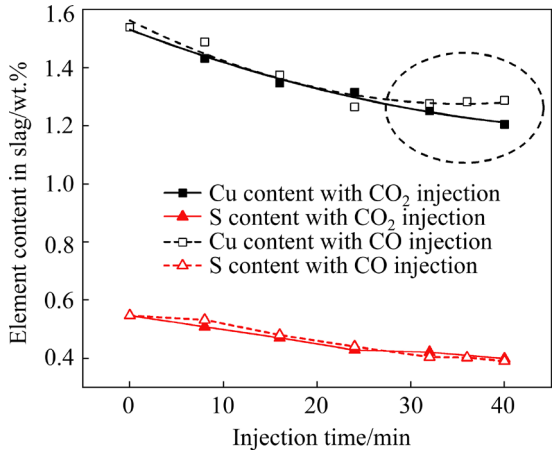

Fig. 9 Variation of Cu and S contents of slag as function of injection time

The distribution ratios of Cu and Fe change based on the injection of different gases, as shown in Fig. 10. During CO_2 injection, the distribution ratio of Cu increases. During oxidation and the removal of sulphur, part of the copper sulphide is oxidised to form metal and enters the matte phase. The removal of sulphur during the oxidation reduces the solubility of Cu in the slag, as reported by scholars [8,30]. In contrast, with the increase in the CO_2 injection time, the distribution ratio of Fe

sharply decreases. During the oxidation, Fe in the matte is oxidised and enters the slag. During CO injection, the distribution ratio of Cu first rapidly increases and then stabilises, whereas the distribution ratio of Fe slowly increases and then remains unchanged. Because the reducibility of CO is relatively weak, CO can reduce a large amount of Cu_2O in the copper slag in the early stage of injection, which leads to a sharp increase in the Cu distribution ratio. Because of the reaction priority of Cu_2O and FeO, a large reduction of iron oxide does not occur in the case of a small amount of injected CO. However, when CO is injected for more than 12 min, the reduction of ferrous oxide starts and the distribution ratio of Cu decreases. After 32 min, the Cu and Fe in the slag are no longer reduced and transferred to the matte.

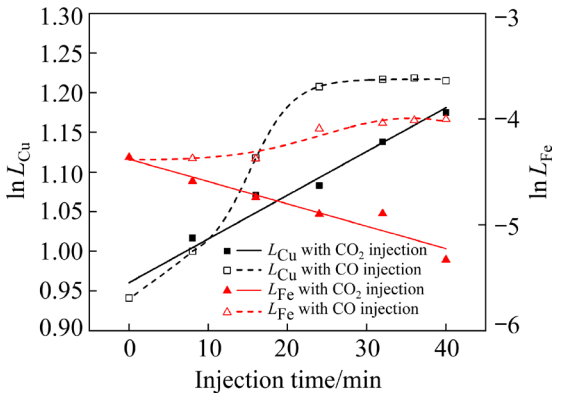

Fig. 10 Distribution ratios of Cu (L_{Cu}) and Fe (L_{Fe}) depending on injection time

The mass of Cu + Fe in the matte and the distribution ratio of arsenic show certain trends (Fig. 11). When large amounts of Fe and Cu enter the matte phase, arsenic is transferred to the matte. The correlation between the distribution ratio of arsenic and the formation mass of Fe + Cu during the reduction is discussed. When Cu and Fe enter the liquid phase, the sulphur content in the matte changes. Figure 11 shows the correlation between the arsenic distribution ratio and the (Cu + Fe) mass fraction. The distribution ratio of arsenic linearly correlates with the mass fraction of (Cu + Fe), which indicates that the dissolution of arsenic into the matte depends on the transport of Cu and Fe during the reduction. In the reduction process, part of the arsenic is absorbed by Cu and Fe and then enters the matte phase, which cannot be removed by gas. The other part of As_2O_3 directly combines with the reactive gas and enters the gas phase. In this process, the reaction and binding species of arsenic in the slag determine its fate. The dissolution of arsenic by Cu–Fe due to the reduction cannot be avoided. YANG et al [31] showed that the volatilization of arsenic was suppressed by a high carbon addition, and the arsenic would be retained in matte.

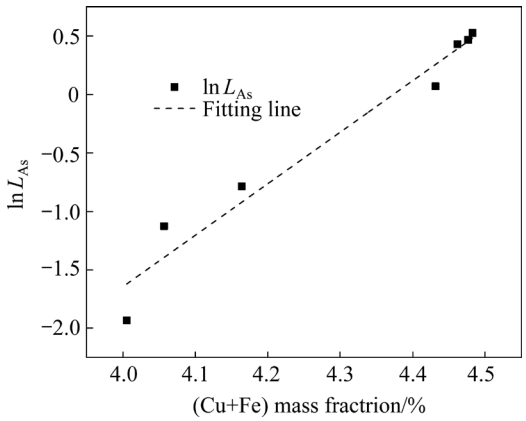

Fig. 11 Correlation between mass fraction of Cu + Fe and distribution ratio of arsenic during CO injection

The increase in the arsenic removal rate through the addition of CO_2 could occur due to the removal of arsenic in the matte phase. Previous studies have observed a slight increase in the arsenic content of the slag when the arsenic is removed from matte during blowing [32]. The dissolution of copper in slag is related to sulphur content [30], and sulphur content improves the sulphide dissolution in slag. These experimental findings indicate several assumptions. First, under the action of CO_2, the sulphur in the molten pool is removed [33]. Second, when the sulphur content is high, arsenic sulphide still dissolves in the slag, and arsenic oxide volatilizes under the action of oxidising gas. This conjecture still needs to be proven by rigorous thermodynamic assessment. At the same time, some scholars have proposed that the content of FeO and oxygen partial pressure in slag has a certain correlation with the activity coefficient of arsenic oxide [34−36], so as to improve the activity coefficient of $AsO_{1.5}$ in slag. This promotes the volatilization of arsenic in the form of oxides.

3.2 Mineral difference of cooled slag

The cooling rate of slag has a substantial impact on the mineralogy and phase composition of

slag. In this study, under the same cooling mode, the mineralogy and phase composition of slag with different gas interventions were compared laterally. Under different gas injection conditions, the phases of the cooled slag sample differ. Figure 12 and Figure 13 show the XRD pattern and morphology of the slag sample, respectively. A large amount of ferric oxide in the molten pool reacts with sulphide or metal under Ar injection, resulting in the transformation of ferric oxide to ferrous oxide. After cooling, magnetite precipitates from the slag. Olivine (Fayalite) is the main phase in the cooling slag and the precipitated magnetite exhibits a connected wedge shape. Many magnetite oxides are formed in the slag and magnetite is precipitated in the form of needle leaves due to the oxidation of CO_2. It is densely dispersed in the ore phase of the cooling slag. Based on the $FeO–Fe_2O_3–SiO_2$ diagram, the main reason for the precipitation of acicular magnetite may be the generation of solid precipitates at 1400 °C, which were uniformly and densely dispersed in the molten pool. With the increase in the ferric oxide content, the melting point of the molten pool increases. During the cooling process, magnetite precipitation cannot nucleate. Under CO injection, magnetite disappears completely. Olivine (Fayalite) is the main phase in the cooled slag. However, there is still a small amount of matte in the slag, which cannot be completely separated in the molten state. The BSD results show that the inclusion of arsenic in the matte causes errors in the experimental data, with the exception of analysis and measurement.

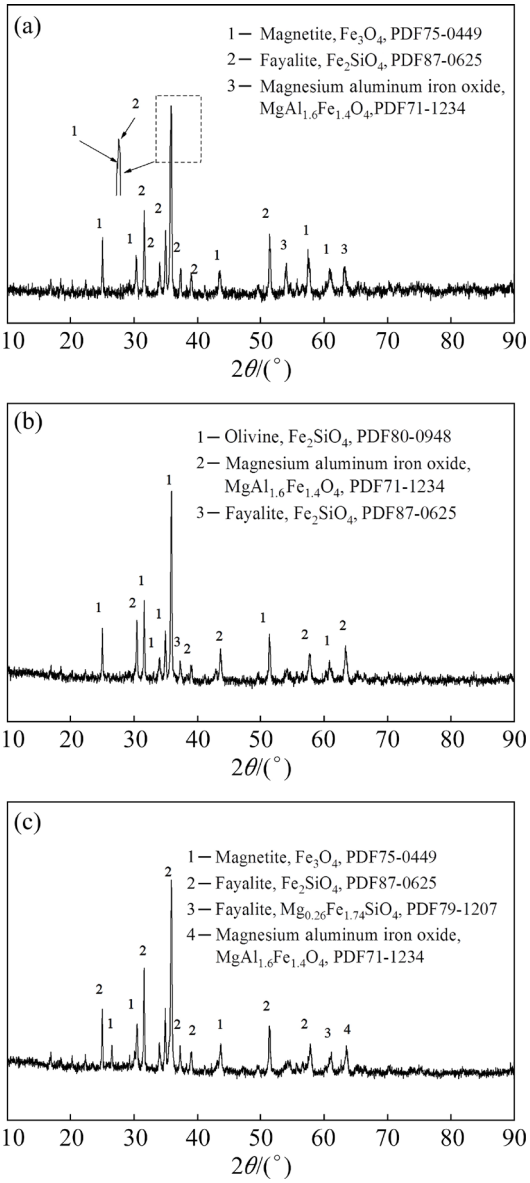

Fig. 12 XRD patterns of slag sample: (a) CO_2 injection, 40 min; (b) CO injection, 40 min; (c) Ar injection, 40 min

3.3 Dissolved forms of arsenic in matte

The distribution of elements in the matte was analysed with EPMA. Subsequently, the formation of arsenic was investigated. As shown in Fig. 14, the dissolution of arsenic in the matte depends on Cu and arsenic is dispersed in the matte as a Cu−As melt. Furthermore, the association of arsenic with sulphur is poor. The transport capacity of copper with respect to arsenic cannot be ignored in the gasification of arsenic in the reducing gas.

3.4 Embedding characteristics of arsenic in slag after different gas injections

The distribution of arsenic in each phase of the slag was measured using EPMA, as shown in Fig. 15. Excluding the Cu−As−S alloy that cannot be separated, the distributions of arsenic and iron in the slag phase have high coincidence, and some studies have similar conclusions [37]. Combined with the distribution of As, Fe, and Si, it could be concluded that arsenic was mainly bound to phases with high iron content, including fayalite, magnetite, and zinc ferrite. Moreover, there was negligible differences in the arsenic content of magnetite, fayalite and silicate (Table S1 in Supplementary materials). In silicate system, the aggregation of lead, antimony and sulphur repelled arsenic, which might be related to the affinity between the elements.

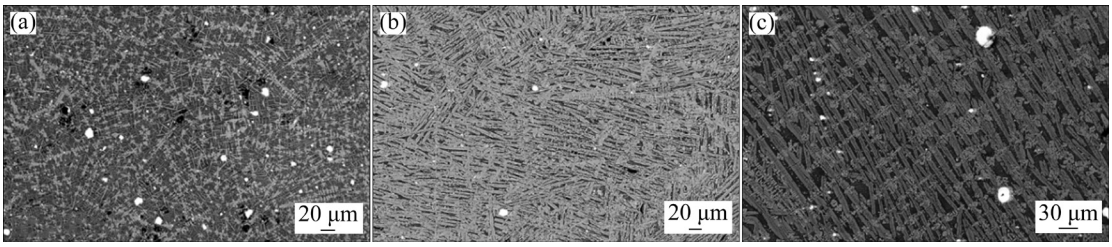

Fig. 13 Morphologies of slag sample by SEM: (a) CO_2 injection, 40 min; (b) CO injection, 40 min; (c) Ar injection, 40 min

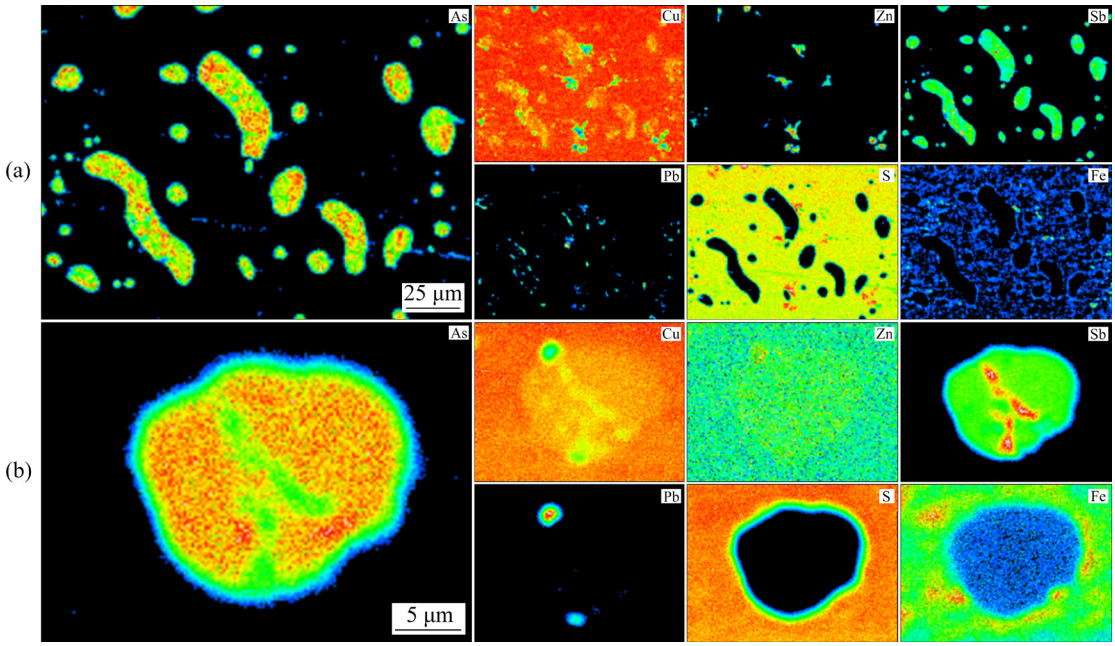

Fig. 14 Morphologies and distributions of elements in obtained matte by EPMA: (a) In low magnification; (b) In high magnification

3.5 Chemical speciation and valence state of arsenic after different gas injections

The XPS data of the experimental slag samples are shown in Fig. 16. XPS peak fitting data are provided in Supplementary materials (Table S2). The main components in the slag were As(V)—O, As(III)—O, arsenic sulphide, and metallic arsenic, similar to the reported studies [8,38,39]. Different scholars have different perspectives about the chemical forms of arsenic in copper slag [14]. The As(V)—O and As(III)—O have notable peaks in the Ar atmosphere. The As(III)—O intensity ratio significantly decreases compared with that of the smelting slag, which is mainly due to the large amount of volatilisation of As_2O_3 from the molten bath due to heating and stirring. The As(V)—O is less volatile. It is more concentrated in the slag in the form of a solid or exists as an arsenate. The intensity ratio of As(V)—O/As(III)—O increases with the injection of CO_2, but the change range is limited. Based on the oxidation ability of CO_2, it cannot infinitely oxidise trivalent arsenic to pentavalent arsenic. Arsenate generally accumulates in magnetite that was formed by the reaction, whereas the ratio of As^{5+}/As^{3+} in the FeO_x–SiO_2 slag system is related to the corresponding oxygen partial pressure ($P(O_2)/P^0$) of the slag system. Arsenic sulphide, As(V)—O, and As(III)—O are the main species under CO injection. Compared with Ar and CO_2, less sulphur is removed, the $P(S_2)/P^0$ ratio of the molten pool system is higher, and parts of the arsenic are present in the form of sulphide in minerals. It is worth noting that although arsenic sulphide is very volatile, arsenic sulphide is still retained in the slag under the action of Ar and CO injection. This may be related to the dissolution of arsenic sulphide in slag or the retention of Cu—As—S compounds in matte without complete separation.

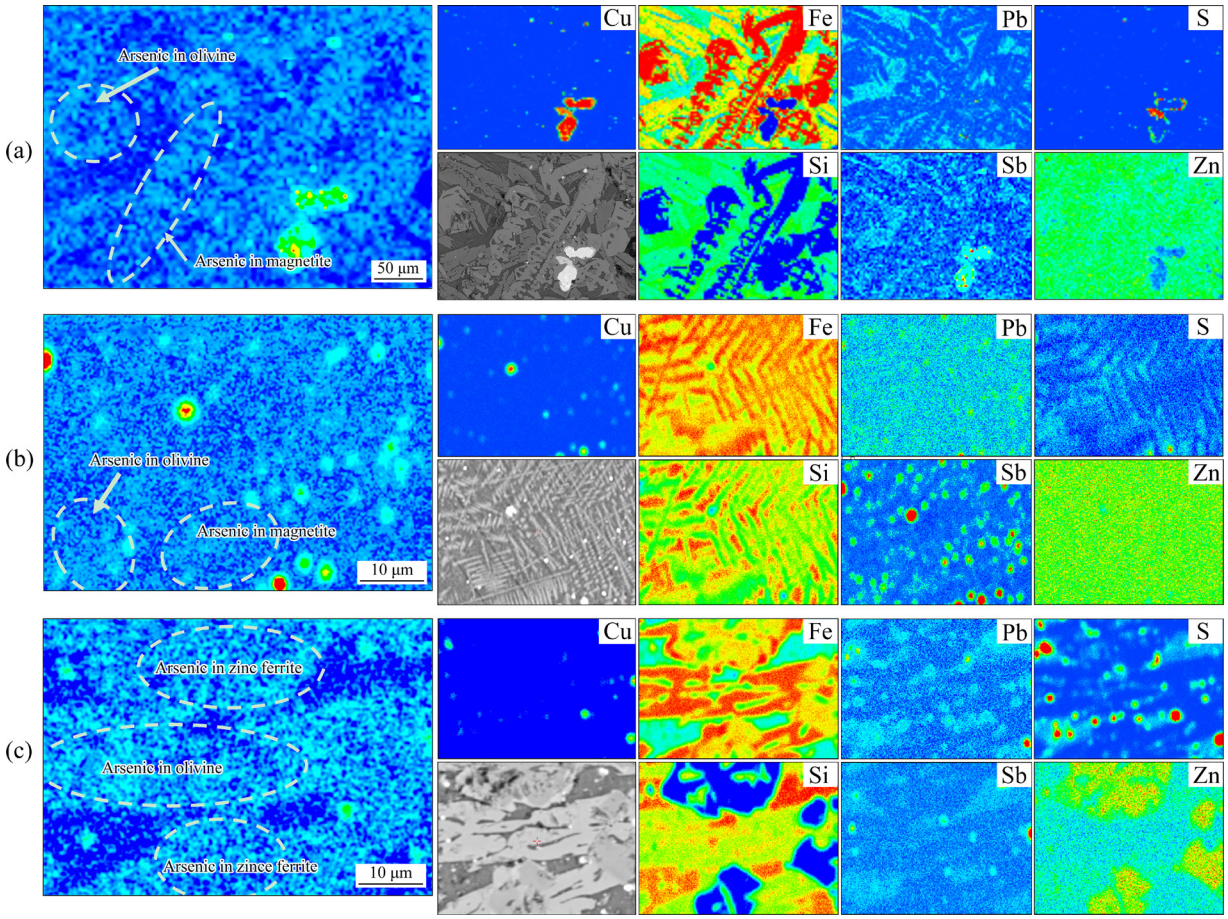

Fig. 15 Distributions of various elements in slag based on EPMA: (a) Ar injection, 40 min; (b) CO_2 injection, 40 min; (c) CO injection, 40 min

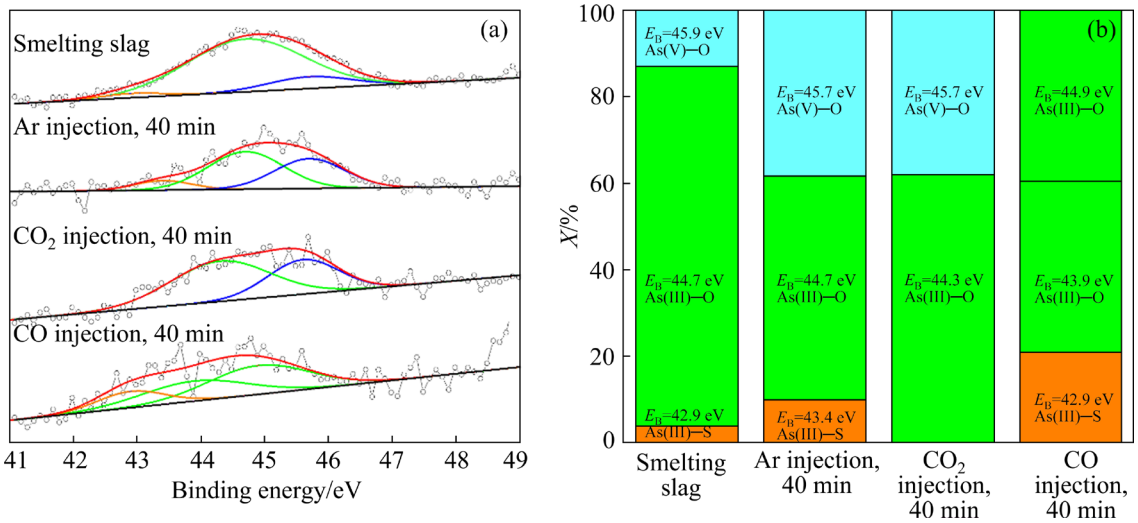

Fig. 16 XPS results for experimental samples: (a) Chemical speciation and valence state of arsenic; (b) Intensity ratio (X)

3.6 Phase composition and morphological characteristics of dust

The XRD data and morphology of dust are shown in Figs. 17 and 18, respectively (Energy spectra are provided in Supplementary materials, Table S3). The volatilisation of arsenic during the heating process cannot be ignored [40,41]. The dust that is generated during gas injection and during the

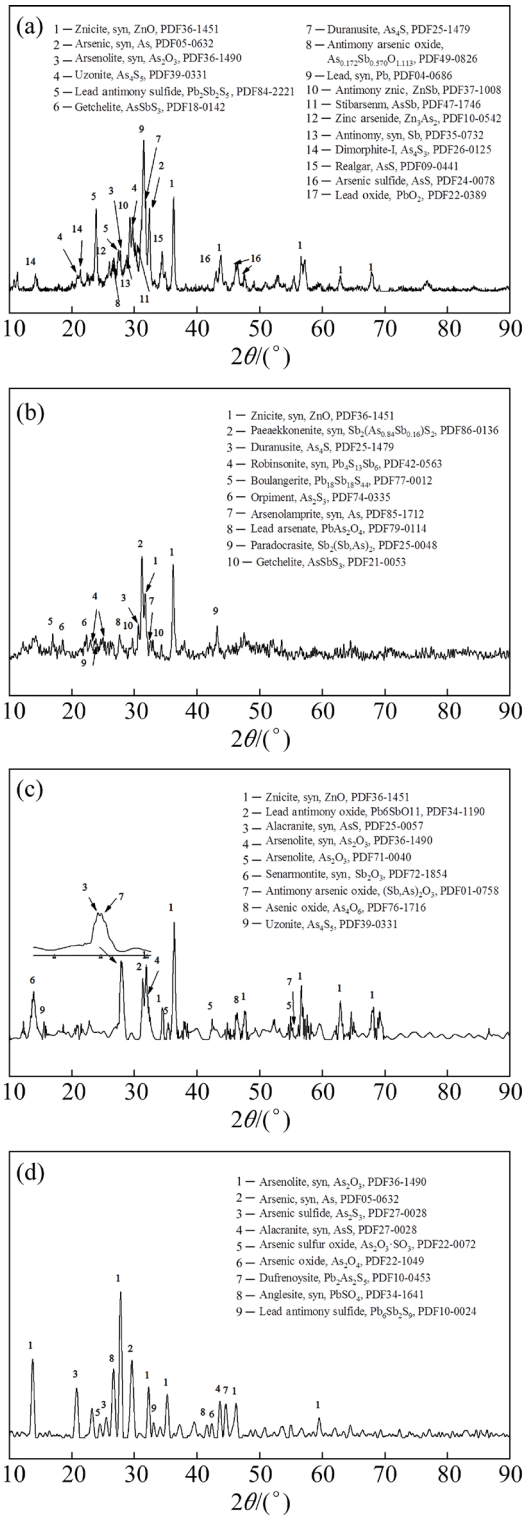

Fig. 17 XRD pattern of received dust: (a) CO injection, 40 min; (b) Ar injection, 40 min; (c) CO_2 injection, 40 min; (d) Solid to melt

heating to the molten state must be collected separately. In the Ar atmosphere, the major volatile phases of arsenic from room temperature to1400 °C are As_2O_3 and As_2S_3. After condensation,

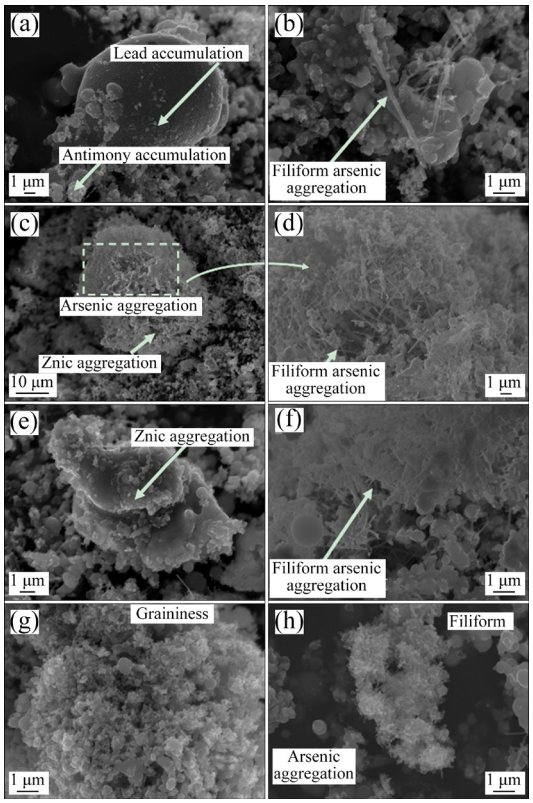

Fig. 18 Micromorphologies of received dust: (a, b) CO injection, 40 min; (c, d) Ar injection, 40 min; (e, f) CO_2 injection, 40 min; (g, h) Solid to melt

arsenic aggregates with graininess and filiform morphology form. After heating to the molten state and stirring with gas, a large amount of ZnO in the molten pool volatilises into the dust. Based on the action of different gases, the ZnO peak can be detected in the XRD data. Under Ar stirring, the main species of arsenic in the dust are arsenic oxide and arsenic sulphide, in addition to minor amounts of elemental arsenic, which is generally composed of volatile Sb. Due to the volatilisation of a large amount of Pb and Sb in the stirring process, several oxides aggregate to form complex compounds, which mostly exist as $Sb_xAs_yO_z$ and $PbAs_2O_4$ polymerised oxides. Note that the volatiles of arsenic are surrounded by ZnO oxide with a filiform morphology under the action of Ar and the volatiles of arsenic do not have a good nucleation ability. Large amounts of Pb and Sb are removed from the molten pool by the injection of CO gas and Pb and Sb are enriched in the dust. The main volatile products of arsenic are As, As_2O_3, and As_xS_y. Because of the volatilisation of Sb, As−Sb compounds are generated during dust nucleation.

Arsenic also has a filiform morphology. Most of the arsenic in the dust collected by condensation nucleates and exhibits a filiform morphology, with diameter below 1 μm and slender shape. The accumulation of arsenic leads to adhesion.

4 Discussion of industrial applications

The predearsenisation of molten copper slag after the smelting process proposed in this study would result in the enrichment of arsenic in the form of dust. Because of the volatility of arsenic, arsenic can be removed from the molten pool based on the stirring effect of inert, oxidising, or reducing gas. When inert gas is used, the arsenic removal simultaneously occurs in the slag system and Cu–As alloy. Therefore, the arsenic content in the tailings and that generated in the raw material recycling process can be reduced. When oxidising gas is injected, the arsenic removal is mainly based on the oxidation and removal of arsenic in Cu–As alloy. The arsenic recycling during matte reuse is inhibited. However, the effect on the arsenic content in tailings is insignificant. The weakly reducing gas plays an important role in the removal of arsenic from the ore phase, greatly reducing the environmental risk of arsenic. After pretreatment, the slag cannot achieve an ideal copper recovery. After the pretreatment, a reducing agent (carbon, oil, etc) is directly added to the molten state to recover copper from the slag. The original one-step smelting reduction method is changed to a two-step process of dearsenisation–copper extraction based on which arsenic can be removed and copper can be simultaneously recovered [42]. Figure 19 shows the method of this process in which we conducted a pilot validation experiment.

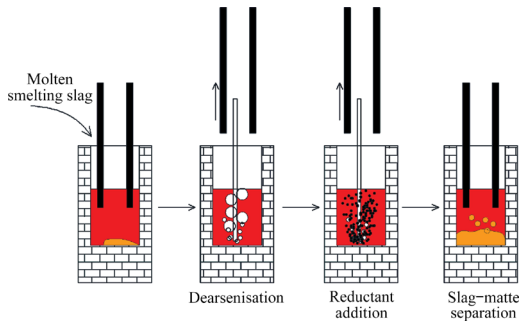

Fig. 19 Pyrometallurgical process for copper recovery based on two-step method

5 Conclusions

(1) The findings of the experiments showed that CO_2 and CO could be used to remove arsenic from molten copper slag. The removal of arsenic by CO_2 mainly occurred in the matte inclusions in the copper slag. The removal of arsenic by CO was mainly related to the arsenic oxides in the slag. The partial pressure of oxygen required for the reduction of arsenic oxides was not low and the reduction reaction occurred readily. Compared with pure Ar injection, the removal rate of arsenic linearly increased with the CO_2 injection time and 51% of arsenic was effectively removed. In contrast, under the action of CO, the removal rate of arsenic was considerably higher and up to 62% of arsenic was removed.

(2) The arsenic removal mechanism differed depending on the gas used for the injection. Arsenic in matte was oxidised and removed by oxidising gas injection and it was difficult for arsenic oxides to dissolve in the slag and directly enter the gas phase. During the injection of reducing gas, the arsenic removal mainly occurred in the slag system. Compared with Ar, the arsenic content in the slag considerably decreased. The injection of different gases led to different compositions and morphologies of the cooled slag samples. It was mainly concentrated in magnetite, fayalite, and zinc ferrite.

(3) The transformation of the arsenic valence state depending on the injection of different gases could be determined. Intensity ratio of As(V)—O/As(III)—O varied depending on the gas used for the injection. Compared with the injection of Ar and CO_2, the arsenic sulphide peak could be observed during the CO injection. Without oxidising gas injection, arsenic sulphide was dispersed in the slag.

(4) The composition of dust differed depending on the gas, but the morphology of arsenic was similar. Arsenic products had a poor nucleation ability and adhered to various compounds with filiform morphology.

(5) Compared to inert gases, if oxidising gas is used for arsenic removal, a large amount of arsenic originally enriched in matte will be removed. After flotation, the arsenic returned to the smelting process will be drastically reduced. If reducing gas is used for dearsenisation, a large amount of arsenic

in the tailings will be removed. When improving the safety of the tailings, it will inevitably increase the arsenic entering the process through matte recovery.

Acknowledgments

This research was supported by the National Natural Science Foundation of China (No. 51674021) and the Major Science and Technology Innovation Project of Shandong Province, China (No. 2019JZZY010358).

Supplementary materials

Supplementary materials in this paper can be found at: http://tnmsc.csu.edu.cn/download/21-p1258-2021-1545-Supplementary_materials.pdf.

References

[1] SHI Cai-jun, MEYER C, BEHNOOD A. Utilization of copper slag in cement and concrete [J]. Resources, Conservation and Recycling, 2008, 52(10): 1115−1120.

[2] TIAN Hong-yu, GUO Zheng-qi, PAN Jian, ZHU De-qing, YANG Cong-cong, XUE Yu-xiao, LI Si-wei, WANG Ding-zheng. Comprehensive review on metallurgical recycling and cleaning of copper slag [J]. Resources, Conservation and Recycling, 2021, 168: 105366.

[3] ZHAO Zong-wen, CHAI Li-yuan, PENG Bing, LIANG Yan-jie, HE Ying-he, YAN Zhi-hao. Arsenic vitrification by copper slag based glass: Mechanism and stability studies [J]. Journal of Non-Crystalline Solids, 2017, 466/467: 21−28.

[4] ZHANG Hui-bin, HE Yu-zheng, HU Jing-jing, WANG Ya-nan, CAO Hua-zhen, ZHOU Jun, ZHENG Guo-qu. Assessment of selective sequential extraction procedure for determining arsenic partitioning in copper slag [J]. Transactions of Nonferrous Metals Society of China, 2020, 30(10): 2823−2835.

[5] CHAN B K C, BOUZALAKOS S, DUDENEY A W L. Integrated waste and water management in mining and metallurgical industries [J]. Transactions of Nonferrous Metals Society of China, 2008, 18(6): 1497−1505.

[6] GUO Xue-yi, CHEN Yuan-lin, WANG Qin-meng, WANG Song-song, TIAN Qing-hua. Copper and arsenic substance flow analysis of pyrometallurgical process for copper production [J]. Transactions of Nonferrous Metals Society of China, 2022, 32(1): 364−376.

[7] YAO Wen-ming, MIN Xiao-bo, LI Qing-zhu, LI Kai-zhong, WANG Yun-yan, WANG Qing-wei, LIU Hui, QU Sheng-li, DONG Zhun-qin, QU Chao, CHEN Tao, SONG Chao. Formation of arsenic−copper-containing particles and their sulfation decomposition mechanism in copper smelting flue gas [J]. Transactions of Nonferrous Metals Society of China, 2021, 31(7): 2153−2164.

[8] NAGAMORI M, MACKEY P J, TARASSOFF P. Copper solubility in FeO—Fe_2O_3—SiO_2—Al_2O_3 slag and distribution equilibria of Pb, Bi, Sb and As between slag and metallic copper [J]. Metallurgical Transactions B, 1975, 6(2): 295−301.

[9] WEISENBERG I J, BAKSHI P S, VERVAERT A E. Arsenic distribution and control in copper smelters [J]. JOM, 1979, 31(10): 38−44.

[10] LONG G, PENG Yong-jun, BRADSHAW D. Flotation separation of copper sulphides from arsenic minerals at Rosebery copper concentrator [J]. Minerals Engineering, 2014, 66/67/68: 207−214.

[11] LEIST M, CASEY R J, CARIDI D. The management of arsenic wastes: Problems and prospects [J]. Journal of Hazardous Materials, 2000, 76(1): 125−138.

[12] MA X, BRUCKARD W J. Rejection of arsenic minerals in sulfide flotation — A literature review [J]. International Journal of Mineral Processing, 2009, 93(2): 89−94.

[13] ZHOU Hui-hui, LIU Gui-jian, ZHANG Li-qun, ZHOU Chun-cai. Mineralogical and morphological factors affecting the separation of copper and arsenic in flash copper smelting slag flotation beneficiation process [J]. Journal of Hazardous Materials, 2021, 401: 123293.

[14] ZHOU Hui-hui, LIU Gui-jian, ZHANG Li-qun, ZHOU Chun-cai, MIAN M M, CHEEMA A I. Strategies for arsenic pollution control from copper pyrometallurgy based on the study of arsenic sources, emission pathways and speciation characterization in copper flash smelting systems [J]. Environmental Pollution, 2021, 270: 116203.

[15] LIAO Ya-long, CHAI Xi-juan, LI Jiang-tao, LI Dong-bo. Study on recovering iron from smelting slag by carbothermic reduction [J]. Advanced Materials Research, 2012, 382: 422−426.

[16] RAJCEVIC H P, OPIE W R. Development of electric furnace slag cleaning at a secondary copper smelter [J]. JOM, 1982, 34(3): 54−56.

[17] ZHANG Huai-wei, SHI Xiao-yan, ZHANG Bo, HONG Xin. Behaviors of the molten copper slags in the vertical electric field [J]. ISIJ International, 2013, 53(10): 1704−1708.

[18] KOMKOV A, KAMKIN R. Reducing treatment of copper smelting slag: Thermodynamic analysis of impurities behavior [J]. JOM, 2011, 63(1): 73−76.

[19] XUE Jian-rong, LONG Dong-ping, ZHONG Hong, WANG Shuai, LIU Li-hua. Comprehensive recovery of arsenic and antimony from arsenic-rich copper smelter dust [J]. Journal of Hazardous Materials, 2021, 413: 125365.

[20] ZHANG Wen-juan, CHE Jian-yong, XIA Liu, WEN Pei-cheng, CHEN Jun, MA Bao-zhong, WANG Cheng-yan. Efficient removal and recovery of arsenic from copper smelting flue dust by a roasting method: Process optimization, phase transformation and mechanism investigation [J]. Journal of Hazardous Materials, 2021, 412: 125232.

[21] XU Zhi-feng, LI Qiang, NIE Hua-ping. Pressure leaching technique of smelter dust with high-copper and high-arsenic [J]. Transactions of Nonferrous Metals Society of China, 2010, 20(S): s176−s181.

[22] TAN Cheng, LI Lei, ZHONG Da-peng, WANG Hua, LI Kong-zhai. Separation of arsenic and antimony from dust with high content of arsenic by a selective sulfidation roasting process using sulfur [J]. Transactions of Nonferrous Metals Society of China, 2018, 28(5): 1027−1035.

[23] GUO Xue-yi, ZHANG Lei, TIAN Qing-hua, YU Da-wei, SHI Jing, YI Yu. Selective removal of as from arsenic-bearing dust rich in Pb and Sb [J]. Transactions of Nonferrous Metals Society of China, 2019, 29(10): 2213−2221.

[24] ZHONG Da-peng, LI Lei. Separation of arsenic from arsenic−

antimony-bearing dust through selective oxidation−sulfidation roasting with CuS [J]. Transactions of Nonferrous Metals Society of China, 2020, 30(1): 223−235.
[25] LIU Wei-feng, FU Xin-xin, YANG Tian-zu, ZHANG Du-chao, CHEN Lin. Oxidation leaching of copper smelting dust by controlling potential [J]. Transactions of Nonferrous Metals Society of China, 2018, 28(9): 1854−1861.
[26] ZIVKOVIC Z, DJORDJEVIC P, MITEVSKA N. Contribution to the examination of the mechanisms of copper loss with the slag in the process of sulfide concentrates smelting [J]. Mining, Metallurgy & Exploration, 2020, 37(1): 267−275.
[27] WEI Guang-sheng, WANG Yun, ZHU Rong, YANG Ling-zhi. Influence of desulfurization with Fe_2O_3 on the reduction of nickel converter slag [J]. Materials, 2020, 13(10): 2423.
[28] MENDOZA D, HINO M, ITAGAKI K. Volatility and vapor pressure measurements of antimony and arsenic components in $CaO−SiO_2−FeO_{1.5}$ slags at 1573 K by transpiration method [J]. Shigen-to-Sozai, 2001, 117(11): 901−906.
[29] SOHN H S, FUKUNAKA Y, OISHI T, SOHN H Y, ASAKI Z. Kinetics of As, Sb, Bi and Pb volatilization from industrial copper matte during $Ar+O_2$ bubbling [J]. Metallurgical and Materials Transactions B, 2004, 35(4): 651−661.
[30] NAGAMORI M. Metal loss to slag. Part I: Sulfidic and oxidic dissolution of copper in fayalite slag from low grade matte [J]. Metallurgical and Materials Transactions B, 1974, 5(3): 531−538.
[31] YANG Wei-chun, TIAN Shun-qi, WU Jian-xun, CHAI Li-yuan, LIAO Qi. Distribution and behavior of arsenic during the reducing−matting smelting process [J]. JOM, 2017, 69(6): 1077−1083.
[32] CHAUBAL P C, NAGAMORI M. Thermodynamics for arsenic and antimony in copper matte converting—Computer simulation [J]. Metallurgical Transactions B, 1988, 19(4): 547−556.
[33] WANG Hong-yang, ZHU Rong, WANG Yun, MI Yu. Experimental study on oxidative desulfurization of molten copper slag by different oxidants [J]. Metallurgical and Materials Transactions B, 2020, 51(2): 543−557.
[34] REDDY R G, FONT J M. Arsenate capacities of copper smelting slags [J]. Metallurgical and Materials Transactions B, 2003, 34(5): 565−571.
[35] CHEN Chun-lin, JAHANSHAHI S. Thermodynamics of arsenic in $FeO_x−CaO−SiO_2$ slags [J]. Metallurgical and Materials Transactions B, 2010, 41(6): 1166−1174.
[36] TAKEDA Y, ISHIWATA S, YAZAWA A. Distribution of minor elements between slag and metallic copper equilibrium study on calcium ferrite slags (4th report) [J]. Journal of the Mining and Metallurgical Institute of Japan, 1984, 100(1152): 103−108.
[37] FU Biao, HOWER J C, LI Shuai, HUANG Yong-da, ZHANG Yue, HU Hong-yun, LIU Hui-min, ZHOU Jun, ZHANG Shi-ding, LIU Jing-jing, YAO Hong. The key roles of Fe-bearing minerals on arsenic capture and speciation transformation during high-as bituminous coal combustion: Experimental and theoretical investigations [J]. Journal of Hazardous Materials, 2021, 415: 125610.
[38] KASHIMA M, EGUCHI M, YAZAWA A. Distribution of impurities between crude copper, white metal and silica-saturated slag [J]. Transactions of the Japan Institute of Metals, 1978, 19(3): 152−158.
[39] JIMBO I, GOTO S, OGAWA O. Equilibria between silica-saturated iron silicate slags and molten Cu−As, Cu−Sb, and Cu−Bi alloys [J]. Metallurgical Transactions B, 1984, 15(3): 535−541.
[40] ZHAO Zong-wen, WANG Zhong-bing, XU Wen-bin, QIN Wei-ning, LEI Jie, DONG Zhun-qin, LIANG Yan-jie. Arsenic removal from copper slag matrix by high temperature sulfide-reduction-volatilization [J]. Journal of Hazardous Materials, 2021, 415: 125642.
[41] WAN Xin-yu, HONG Lu-kuo, QI Yuan-hong, GAO Jian-jun. Removal of arsenic during iron extraction from waste copper slag [J]. Transactions of the Indian Institute of Metals, 2020, 73(11): 2683−2691.
[42] WANG Hong-yang, ZHU Rong, DONG Kai, ZHANG Si-qi, ZHAO Rui-min, JIANG Zhen-qiang, LAN Xin-yi. An experimental comparison: Horizontal evaluation of valuable metal extraction and arsenic emission characteristics of tailings from different copper smelting slag recovery processes [J]. Journal of Hazardous Materials, 2022, 430: 128493.

不同喷吹气体对铜冶炼熔渣中砷气化脱除的影响

王宏阳[1,2]，朱 荣[1,2]，董 凯[1,2]，张思奇[3]，王 云[4]，兰昕怡[5]

1. 北京科技大学 冶金与生态工程学院，北京 100083；
2. 北京科技大学 北京高端金属材料特殊熔炼与制备重点实验室，北京 100083；
3. 北京科技大学 土木与资源工程学院，北京 100083；
4. 中国恩菲工程技术有限公司，北京 100038；5. 北京科技大学 自动化学院，北京 100083

摘 要：为了减少铜熔炼渣中砷所带来的环境问题，提出一种基于气体喷吹脱除熔融铜渣中砷的方法，期望在铜回收工艺前将铜熔炼渣中的砷尽可能以粉尘的形式富集。对比惰性气体、氧化性气体和还原性气体对熔渣中砷脱除的影响。氧化性气体 CO_2 氧化夹杂冰铜中的砷及砷硫化物，并充当气体载体将砷氧化物带出熔池。还原性气体 CO 可以将 $FeO_x−SiO_2$ 熔渣中的砷氧化物还原，并使其挥发至气相，可以实现 60%以上的砷脱除率。该研究为熔炼渣中砷脱除提供指导。

关键词：铜熔炼渣；砷脱除；气体喷吹；污染物控制

(Edited by Bing YANG)